

Vector Meson Spectrum from top-down Holographic QCD

Mohammed Mia*

*Department of Physics and Astronomy, Purdue University,
525 Northwestern Avenue, West Lafayette, IN 47907, USA*

Keshav Dasgupta,[†] Charles Gale,[‡] Michael Richard,[§] and Olivier Trottier[¶]

Department of Physics, McGill University, 3600 University Street, Montreal, QC, H3A 2T8, Canada

(Dated: November 27, 2024)

We elaborate on the brane configuration that gives rise to a QCD-like gauge theory that confines at low energies and becomes scale invariant at the highest energies. In the limit where the rank of the gauge group is large, a gravitational description emerges. For the confined phase, we obtain a vector meson spectrum and demonstrate how certain choice of parameters can lead to quantitative agreement with empirical data.

I. INTRODUCTION

Quantum Chromo-Dynamics (QCD) is the accepted gauge theory of the strong interaction, and its degrees of freedom are the fermionic quarks (and anti-quarks) and the bosonic gluons. The fact that the gluon gauge fields admit self-interaction creates a scale-dependent coupling: at short distances, smaller than that of a proton, a quark-antiquark pair experiences a Coulomb-like potential while at larger distances the pair binds in a field configuration that is like that of a flux tube. In the regime where the coupling between partons becomes large, calculations of the low energy properties of QCD have traditionally relied either on large numerical simulation of the theory, discretized on a space-time lattice (“lattice QCD”), or on the use of effective theories based on some of the fundamental symmetries of QCD. However, a new class of approaches that have generated great interest is that based on the concept of holographic duality as expressed through the famous AdS/CFT correspondence [1]. A powerful feature of such dualities is that even though the field theory sector might be strongly coupled, its gravity dual can be treated in perturbation theory. This opens the tantalizing prospect of being able to treat systems interacting through low-energy QCD analytically, at least to some extent. Theories that attempt to realize this potential are globally labelled AdS/QCD. Even through no formal gravity dual of QCD is known, several models use holographic techniques to arrive at “QCD-like” field theories, at least to explain the infrared (IR) dynamics. One important example being the Klebanov-Strassler model [2]. Bottom-up approaches are phenomenologically based and are not as such compelled by the rules of string theory. Top-down approaches start with gauge theory arising from open strings ending on

branes and then study the dual closed string sector described by classical gravity. Such an approach, that in fact covers the regime from low to high energies, is used in this work; the next section describes this top-down model. Then, we construct a pseudo-QCD action from our gravity dual, and calculate the vector meson mass spectrum. We compare our results with those obtained using the Sakai-Sugimoto model, and also with experimentally measured masses. We end with a conclusion.

II. BRANE CONFIGURATION

We start with coincident N Dirichlet three-branes ($D3$ branes) and M Dirichlet five-branes ($D5$ branes) at the tip of a cone [See Figure 1] and add M anti-five branes separated from each other and from the $D3/D5$ branes [See Figure 1]. To obtain this separation, we must blow up one of the S^2 's at the tip and give it a finite size. The separation gives masses Λ_0 to the $D5/\bar{D}5$ strings and at scales $\Lambda < \Lambda_0$, the gauge group is $SU(N+M) \times SU(N) \times U(1)^M$ where the additional $U(1)$ groups arise from the massless strings ending on the $\bar{D}5$ -branes spread above the equator of the S^2 . The $SU(M+N)$ sector has $2N$ effective flavors while the $SU(N)$ sector has $2(N+M)$ effective flavors thus it is dual to the $SU(N-M) \times SU(N)$ gauge theory under a Seiberg duality. Under a series of such dualities, which is called cascading, at the far IR region the gauge theory can be described by $SU(M) \times SU(K)$ group, where $N = lM + K$, $l, 0 \leq K < M$ are positive integers. Now the number of ‘actual’ $D3$ branes N is no longer the relevant quantity, rather $N \pm pM$ where p is an integer describes the $D3$ brane charge. We take $K = 0$ in all our analysis, so at the bottom of the cascade, we are left with $\mathcal{N} = 1$ SUSY $SU(M)$ strongly coupled gauge theory which looks very much like strongly coupled SUSY QCD.

At high energies $\Lambda \gg \Lambda_0$, $D5/\bar{D}5$ strings are excited and we have $SU(N+M) \times SU(N+M)$ gauge theory. Essentially M pairs of $D5/\bar{D}5$ branes with fluxes are equivalent to M number of $D3$ branes and hence they contribute an additional M units of $D3$ charge, resulting in

* mmia@purdue.edu

† keshavhep.physics.mcgill.ca

‡ gale@physics.mcgill.ca

§ michael.richard@mail.mcgill.ca

¶ olivier.trottier@mail.mcgill.ca

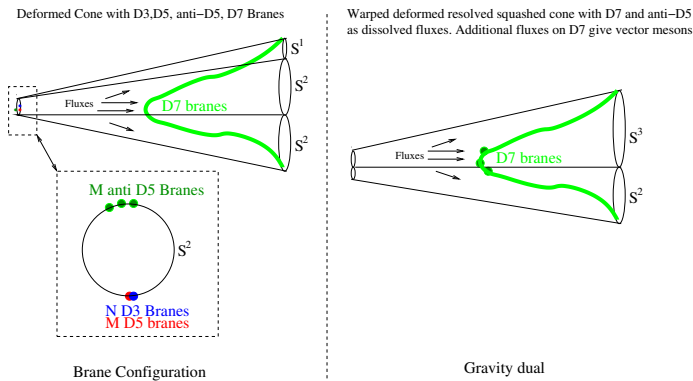


FIG. 1. Brane configuration and the dual gravity in the extremal limit for a UV regular theory. The anti-branes should be thought of as spread above the equator of the resolved sphere although the branes are all localised at the south pole of the sphere. The manifolds appearing on both sides of the duality are in general non-Kähler manifolds although in the limit of vanishing resolution and squashing they become Kähler Calabi-Yau spaces.

$SU(N+M) \times SU(N+M)$ conformal theory. In summary, for $\Lambda \ll \Lambda_0$, i.e. at low energy, we have $SU(M)$ gauge group that confines while at high energy $\Lambda \gg \Lambda_0$, we have a conformal field theory with two copies of $SU(N+M)$ group. Pure glue QCD, with large number of colors, confines in the IR and becomes conformal at the UV – thus the brane setup gives rise to a QCD like gauge theory. To add flavor, we can add D7 branes but the overall setup does not change – we still have UV conformal gauge theory that confines in the IR. In fact the walking RG flow in the UV due to the flavor seven-branes match up precisely with the IR RG flow leading to confinement.

Now of course the presence of anti branes will create tachyonic modes and system will be unstable. To stabilize the system against gravitational and RR forces, we need to add world volume fluxes on the $D5/\bar{D}5$ branes. Alternatively, we can introduce D7 branes and absorb the anti-D5 branes as gauge fluxes on the D7 branes. Then a stable configuration of D7 branes with gauge fluxes in the presence of coincident D3/D5 branes will be equivalent to stable configuration of coincident D3/D5 branes and anti-D5 along with D7 branes. More details on the stabilization procedure will be discussed in [3].

Observe that D7 branes also introduce fundamental matter and with world volume fluxes on Minkowski directions, they give rise to vector mesons as we shall see shortly. In summary, D7 branes play two crucial roles: they source anti-D5 charge and produce vector mesons for the four dimensional gauge theory. In principal different embeddings can be used for distinct purposes. In Figure 1, we have sketched a generic D7 embedding. Introducing various fluxes will determine the precise embedding and in turn modify the gauge theory.

III. GRAVITY DESCRIPTION

When the 'tHooft coupling for the gauge theory is large, which can be achieved for example with large M , we can obtain a classical gravitational description for the gauge theory arising from the above brane setup. The gravity action arises from low energy limit of type IIB critical superstring action with localized sources given as:

$$\begin{aligned}
 S_{\text{total}} &= S_{\text{SUGRA}} + N_f S_{Dp} \\
 S_{\text{SUGRA}} &= \frac{1}{2\kappa_{10}^2} \int d^{10}x \sqrt{G} \left(R + \frac{\partial_M \tau \partial^M \bar{\tau}}{2|\text{Im}\tau|^2} - \frac{|\tilde{F}_5|^2}{4 \cdot 5!} \right. \\
 &\quad \left. - \frac{G_3 \cdot \bar{G}_3}{12\text{Im}\tau} \right) + \frac{1}{8i\kappa_{10}^2} \int \frac{C_4 \wedge G_3 \wedge \bar{G}_3}{\text{Im}\tau} \\
 S_{Dp} &= - \int d^{p+1} \sigma T_p e^{\frac{\phi(p+1)}{4}} \sqrt{-f} \left(1 + e^{-\phi} \frac{1}{4} \tilde{F}^{ab} \tilde{F}_{ab} \right) \\
 &\quad + \mu_p \int (C \wedge e^{\tilde{F}})_{p+1} \tag{3.1}
 \end{aligned}$$

where N_f is number of Dp branes, $\tau = C_0 + ie^{-\phi}$, $F_1 = dC_0$ and $G = \det g_{PQ}$, $P, Q = 0, \dots, 9$ with g_{PQ} is the metric in Einstein frame. Also $G_3 = F_3 - \tau H_3$, $f = \det f_{ab}$ with $f_{ab} = g_{PQ} \partial_a X^P \partial_b X^Q$. Note that $\tilde{F}_{ab} = F_{ab} + B_{ab}$, F_{ab} is the world volume flux, $B_{ab} = B_{PQ} \partial_a X^P \partial_b X^Q$ with B_{PQ} being the NS-NS two form and \tilde{F}_{ab} is raised or lowered with the pullback metric f_{ab} . The background warped metric takes the following familiar form

$$\begin{aligned}
 ds^2 &= g_{PQ} dx^P dx^Q \equiv g_{\mu\nu} dx^\mu dx^\nu + g_{mn} dx^m dx^n \\
 &= -e^{2A+2B} dt^2 + e^{2A} d\vec{x}^2 + e^{-2A-2B} \tilde{g}_{mn} dx^m dx^n \tag{3.2}
 \end{aligned}$$

where $d\vec{x}^2 = dx^2 + dy^2 + dz^2$, $\mu, \nu = 0, \dots, 3$, $m, n = 4, \dots, 9$ and the internal unwarped metric is given by $\tilde{g}_{mn} \equiv \tilde{g}_{mn}^0 + \tilde{g}_{mn}^1$. Here \tilde{g}_{mn}^0 describes the base of a deformed cone with or without resolution or squashing, while \tilde{g}_{mn}^1 is the perturbation due to the presence of fluxes and localized sources [19]. A resolved-deformed cone refers to the base where cycles never go to zero size and squashing describes the deviation of shapes from an ordinary n -sphere. Resolution, deformation and squashing parameters are dual description of a particular expectation value of gauge invariant combinations of bifundamental matter fields at the far IR of the gauge theory. The right figure in Figure 1 is a sketch of a warped resolved-deformed and squashed conifold which captures the most general dual gravity corresponding to a confining gauge theory with some expectation value of baryonic operators. When resolution and squashing are set to zero, we also have non-zero expectation values, provided we consider deformed cone just like Klebanov-Strassler [2]. When we are away from the resolved-deformed tip of the cone and there is no squashing, \tilde{g}_{mn}^0 is the metric of $R^1 \times T^{1,1}$.

The action (3.1) in the absence of any localized sources can describe the gauge theory arising from the brane

setup of Figure 1, provided $G_3 \neq 0$. When $G_3 = 0$, one can obtain an $AdS_5 \times T^{1,1}$ geometry which describes a CFT [4]. The presence of localized sources allow us to patch together a warped deformed conifold geometry with $G_3 \neq 0$ at small radial distances to an asymptotically $AdS_5 \times T^{1,1}$ geometry. The localized sources have to alter G_3 , so we look for $D5$ or anti- $D5$ branes. We can also dissolve these branes as gauge fluxes on $D7$ branes. We take the latter approach since it is easier to find stable $D7$ brane embeddings.

The $D7$ branes fill up Minkowski space (t, x, y, z) , stretching along radial r direction and filling up S^3 inside the $T^{1,1} = S^3 \times S^2$. In the absence of resolution and squashing, [5] proposed $D7$ branes embeddings that source world volume fluxes \widetilde{F}_2 inducing anti- $D5$ charge. There were two branches of the $D7$ brane and the world volume flux on each branch modifies the background RR and NS-NS three form flux, resulting in the following fluxes

$$F_3 = \frac{M\alpha'}{2}\omega_3 + 4\kappa_{10}^2 \widetilde{M} N_f \alpha' \mu_7 \left(F(r)\widetilde{\omega}_3^{-1} + H(r)\widetilde{\omega}_3^2 \right)$$

$$H_3 = \frac{*_6(e^B F_3)}{\text{Im}\tau} \quad (3.3)$$

where $*_6$ is the hodge star for the metric g_{mn} . The definitions of the three forms $\omega_3, \widetilde{\omega}_3^{-1}, \widetilde{\omega}_3^2$ and of the scalar functions $F(r), H(r)$ can be found in [5] (see also earlier works [6–8]). The effective number of $D5$ branes in the dual gauge theory can be obtained using Gauss' law:

$$M_{\text{eff}}^{\text{total}} = \int F_3 \quad (3.4)$$

For a given value of M , we can choose \widetilde{M} such that

$$\int_{r \rightarrow \infty} F_3 = 0 \quad \Rightarrow \quad M_{\text{eff}}^{\text{total}}(r \rightarrow \infty) = 0 \quad (3.5)$$

Since the radial coordinate r is dual to the energy scale of the gauge theory, we find that the total $D5$ brane charge vanishes in the far UV and we are left only with $D3$ branes. Thus For $r < r_0$, that is $\Lambda < \Lambda_0$, one finds using (3.3) that $M_{\text{eff}}^{\text{total}}(\Lambda < \Lambda_0) \sim M$ i.e. we have M units of $D5$ charge.

The introduction of r_0 gives rise to a scale and we divide the geometry into three regions: a classification that will be particularly useful in studying meson spectrum. Region I: $r < r_0$; Region II: $r \sim r_0$; Region III: $r \gg r_0$

A. Confinement and meson spectrum

The form of the metric (3.2) describes a manifold X with or without a black hole. When $B = 0$, we have a geometry without a black hole while in the presence of a black hole, we have a horizon with radial location $r = r_h$ such that $e^{B(r_h)} = 0, e^{2A(r_h)} \neq 0$. The temperature of the

gauge theory dual to X is determined by the singularity structure of X in the following way: analytically continue $\tilde{\tau} = -it$ to obtain the Euclidean metric where $\tilde{\tau} \in [0, \beta]$. Then temperature is given by $T^{-1} = \beta$. In the presence of a black hole, X is singular and removing the singularity fixes the period β . Thus for a black hole geometry, the temperature is related to the horizon. On the other hand, in the absence of a black hole we pick any value of β since we consider warp factors $e^{-4A} = h$ to be regular on X . If we denote the ‘vacuum’ geometry without a black hole by X^1 with on-shell action \mathcal{S}^1 and black hole geometry by X^2 with on-shell action \mathcal{S}^2 , then at a given temperature the geometry with smaller value of on-shell action will be preferred. At $T = T_c$, $\Delta\mathcal{S} \equiv \mathcal{S}^2 - \mathcal{S}^1 = 0$ and we have a phase transition. At $T < T_c$, $\Delta\mathcal{S} > 0$ and X^1 is preferred [10][11][5][12]. Since there is no black hole, X^1 corresponds to zero entropy and confinement. On the other hand for $T > T_c$, $\Delta\mathcal{S} < 0$ and black hole geometry is preferred. Since the black hole has non-zero entropy, the gauge theory is in the deconfined phase and $T = T_c$ corresponds to confinement/deconfinement transition temperature.

Thus at small temperatures $T < T_c$, we can consider the ‘vacuum’ geometry without a black hole since it describes the confined phase. We can obtain the meson spectrum by introducing additional $D7$ branes embedded as probes in the geometry with metric (3.2) in the limit $B = 0$. Note that these probe $D7$ branes differ from the $D7$ branes considered in [5]. The additional probe branes with world volume fluxes in Minkowski directions give rise to QCD like vector mesons. The world volume fluxes on the background $D7$ branes have no legs in the Minkowski directions and they represent dissolved anti- $D5$ branes necessary for a UV complete theory.

Before going into the details of the probe brane embedding, observe that the energy scale Λ_0 corresponding to r_0 provides us a notion of UV and IR energies. Since mesons appear at low energies, we expect the spectrum to be sensitive to Region I with $r < r_0$ and the characteristic mass scale for the mesons to be set by $r_c < r_0$. This mass scale manifests itself in the dual geometry via $D7$ embedding that stretches from $r = \infty$ to $r = r_c$. Now if we consider the trivial embedding where the pull back metric is the spacetime metric and the brane is a point in the transverse directions with embedding function being constant, then the brane will slide down to the region $r < r_c$ due to gravitational pull. If we consider the brane to have some shape i.e. the embedding function is not a constant, then it will be possible for it to end at r_c , just like the U shaped embedding in [14]. However, the spectrum analysis becomes quite involved for a non-trivial embedding, since the gauge fluxes and embedding will be coupled.

One alternative to avoid such complications is to cut off the geometry at $r = r_c$ and only consider the $r \geq r_c$ region. In this scenario, the constant embedding $D7$ brane will extend from $r = \infty$ to $r = r_c$ and r_c will provide the characteristic scale of the mesons. For instance, all

the meson masses will be expressed in units of r_c . In the following analysis, we will introduce r_c as a cutoff in the geometry which essentially acts as an IR cutoff in the gauge theory. The cutoff geometry will have the same form (3.1) as it's action with the boundary condition for metric and fluxes at $r = r_c$ consistent with the bulk solution without the cutoff.

To draw a parallel with the celebrated Sakai-Sugimoto model [15, 16], we T-dualize the metric (3.2) along the ψ coordinate of the conifold geometry and analyze the DBI action of a single D6 brane. We pick world volume parametrization $(\sigma^0, \dots, \sigma^6) = (t, x, y, z, r, \phi_2, \theta_2)$ and the brane is a point inside S^3 with the embedding: $(\theta_1, \phi_1, \psi) = (0, 0, \psi(r))$. The induced metric and B -field on the D6 world volume are:

$$\begin{aligned} f_{ab}dX^a dX^b &= \frac{\eta_{\mu\nu}dx^\mu dx^\nu}{\sqrt{h(r)}} + \frac{9L^4}{r^2\sqrt{h(r)}}\psi'(r)^2 dr^2 \\ &+ \sqrt{h(r)} [dr^2 + r^2 (d\theta_2^2 + (u + \sin(\theta_2))^2 d\phi_2^2)] \\ B_2 &= 3g_s M \log(r/r_c) \sin(\theta_2) d\theta_2 \wedge d\phi_2 \\ &+ 2L^2 \psi'(r) \cos(\theta_2) dr \wedge d\phi_2 \\ e^{-\phi(r)} &= \frac{h(r)^{\frac{1}{4}} r}{6g_s}, \quad h(r) = \frac{L^4 \left(1 + \frac{3g_s M^2 \log(r/r_c)}{2\pi N}\right)}{4r^4} \end{aligned} \quad (3.6)$$

where $L^4 = 27\pi N\alpha'^2$ and u is a *squashing* parameter describing a squashed sphere at the base of the cone. Since we will only consider $u \ll 1$, we do not show its dependence on the RR fields; and (B_2, ϕ) are kept independent of u . Also note that the warp factor $h(r)$ above is only valid for Region I and we are considering a region away from resolved/deformed base. Thus essentially we consider T-dual of the warped squashed $T^{1,1}$. Solving the embedding equation for $\psi(r)$, one finds that $\psi(r) = c$ (constant) is a solution [3]. For the study of meson spectrum one needs to study fluctuations of embedding for which more convenient coordinates are (Y, Z) :

$$\begin{aligned} Y &= \rho \cos(\theta), & Z &= \rho \sin(\theta) \\ \rho &= \sqrt{Y^2 + Z^2}, & \theta &= \arctan\left(\frac{Z}{Y}\right) \\ r &= r_c e^\rho, & \psi &= \frac{2c}{\pi} \theta \end{aligned} \quad (3.7)$$

In this new coordinate system, the constant embedding is described by $Y = 0$. Also note that the coordinate transformation makes the IR cutoff $r = r_c$ manifest since in the new coordinate $\rho \geq 0$ spans the entire cutoff geometry. Finally, if r_c is bigger than the deformation parameter that appears in Klebanov-Strassler theory [20], we effectively consider mesons heavier than the confinement scale.

1. Vector Mesons Action

The vector mesons arises by considering gauge flux (A_M) along the Minkowski (t, x, y, z) and Z directions.

$$\begin{aligned} A_M &= \begin{cases} A_\mu(x^\mu, Z) & \text{when } M = \mu \in \{t, x, y, z\} \\ A_Z(x^\mu, Z) & \text{when } M = Z \\ 0 & \text{when } M \in \{\theta_2, \phi_2\} \end{cases} \\ F_{MN} &= \partial_M A_N - \partial_N A_M \end{aligned} \quad (3.8)$$

Looking at terms quadratic in F_{MN} in the DBI action, we have:

$$\begin{aligned} S_{D6} &= -T \int d^4x dZ d\theta_2 d\phi_2 e^{-\phi(r(0,Z))} \sqrt{-\det(g_6 + \mathcal{B}_6)} \\ &= -(2\pi\alpha')^2 T \int d^4x dZ \left(v_1(Z) \eta^{\mu\nu} F_{\mu Z} F_{\nu Z} \right. \\ &\quad \left. + v_2(Z) \eta^{\mu\nu} \eta^{\rho\sigma} F_{\mu\rho} F_{\nu\sigma} + \dots \right) \end{aligned} \quad (3.9)$$

where $\mathcal{B}_6 \equiv B_6 + 2\pi\alpha'$; and $v_1(Z)$ and $v_2(Z)$ are even functions of Z , which also have non-trivial dependence on u, g_s and M . The algebraic expressions of these functions can be found in [3].

We now expand A_μ and A_Z in eigenmodes using two sets of eigenfunctions $\{\alpha_n(Z), n \geq 1\}$ and $\{\beta_n(Z), n \geq 0\}$

$$\begin{aligned} A_\mu(x^\mu, Z) &= \sum_{n=1}^{\infty} B_\mu^{(n)}(x^\mu) \alpha_n(Z) \\ A_Z(x^\mu, Z) &= \sum_{n=0}^{\infty} \varphi^{(n)}(x^\mu) \beta_n(Z) \end{aligned} \quad (3.10)$$

Focusing on terms proportional to α_n^2 , we obtain terms reminiscent of the vector mesons terms of QCD.

$$\begin{aligned} S_{\alpha_n^2} &= -(2\pi\alpha')^2 T \int d^4x dZ \sum_{m,n} [v_2(Z) F_{\mu\nu}^{(n)} F^{\mu\nu(m)} \alpha_n \alpha_m \\ &\quad + v_1(Z) B_\mu^{(m)} B^{\mu(n)} \dot{\alpha}_m \dot{\alpha}_n] \end{aligned} \quad (3.11)$$

We will now impose the following conditions on α_n ,

$$-\partial_Z (v_1(Z) \partial_Z \alpha_n) = 2v_2(Z) m_n^2 \alpha_n \quad (3.12)$$

$$(2\pi\alpha')^2 T \int dZ v_2(Z) \alpha_m \alpha_n = \frac{1}{4} \delta_{mn} \quad (3.13)$$

where $m_n^2 \equiv \lambda_n \mathcal{M}^2$ is the effective squared-mass of each vector meson and λ_n is the eigenvalue of the corresponding mode. As expected, the mass scale \mathcal{M}^2 is given by $\frac{r_c^2}{4\pi N\alpha'^2}$. From the last two equations, we can derive the following identity:

$$(2\pi\alpha')^2 T \int dZ v_1(Z) \dot{\alpha}_m \dot{\alpha}_n = \frac{1}{2} m_n^2 \delta_{mn} \quad (3.14)$$

Using the above relation, the action (3.11) takes the form resembling QCD.

$$S_{QCD} = - \sum_{n=1}^{\infty} \int d^4x \left(\frac{1}{4} F_{\mu\nu}^{(n)} F^{\mu\nu(n)} + \frac{1}{2} m_n^2 B_\mu^{(n)} B^{\mu(n)} \right) \quad (3.15)$$

and thus m_n can indeed be identified with the vector meson mass.

2. Vector Mesons Spectrum

We now solve the eigenvalue equation (3.12) by using simple perturbation techniques with $\delta \equiv \frac{g_s M^2}{N}$ as the controlling parameter. We introduce some notation to write the problem in terms of a differential operator \mathbf{H}_v acting on its eigenfunctions α_n [3].

$$\begin{aligned}
(3.12) \rightarrow \mathbf{H}_v |\alpha_n\rangle &= \lambda_n |\alpha_n\rangle \\
\mathbf{H}_v &\equiv -\frac{v_1(Z)}{2\mathcal{M}^2 v_2(Z)} \left(\partial_Z^2 + \frac{v_1'(Z)}{v_1(Z)} \partial_Z \right) \\
f(Z) &\equiv 4(2\pi\alpha')^2 T v_2(Z) \\
\langle \alpha_m | \alpha_n \rangle &\equiv \int_{\mathbb{R} \setminus \{0\}} dZ f(Z) \alpha_m \alpha_n = \delta_{mn} \quad (3.16)
\end{aligned}$$

We can now solve eq. (3.16) up to first order in δ obtaining the eigenfunctions and eigenvalues [3]. We impose that the eigenfunctions be normalizable so that the orthogonality condition in (3.16) is satisfied. At zeroth order in δ , the eigenfunctions are given in terms of Bessel's functions of the first kind.

$$\alpha_n^{(0)}(Z) = C e^{-|Z|} J_1 \left(\sqrt{\lambda_n} e^{-|Z|} \right) \quad (3.17)$$

C is determined by using the zeroth-order normalization condition. The eigenvalues are obtained by solving the following equations, which we expect for odd and even functions. These conditions also guarantee perfect orthogonality of the eigenfunctions:

$$\alpha_n^{(0)}(0, \lambda_n) = 0 \quad (\text{Odd functions}) \quad (3.18)$$

$$\partial_Z \alpha_n^{(0)}(0, \lambda_n) = 0 \quad (\text{Even functions}) \quad (3.19)$$

For odd functions, we also add an extra $\text{sgn}(Z)$ to make them truly odd. Using the same indexing as Sakai & Sugimoto, the eigenfunctions are summarized as follows:

$$\alpha_{2n+1}^{(0)}(Z) = C e^{-|Z|} J_1 \left(\sqrt{\lambda_{2n+1}} e^{-|Z|} \right) \quad (3.20)$$

$$\alpha_{2n}^{(0)}(Z) = C \text{sgn}(Z) e^{-|Z|} J_1 \left(\sqrt{\lambda_{2n}} e^{-|Z|} \right) \quad (3.21)$$

Now the first-order correction to the eigenvalues of eq.(3.16) is given by the well-known formula in perturbation theory and are expressed here as [3]:

$$\begin{aligned}
\lambda_n^{(1)} &= \langle \alpha_n^{(0)} | \mathbf{H}_v^{(1)} | \alpha_n^{(0)} \rangle^{(0)} \\
\mathbf{H}_v^{(1)} &= \frac{3e^{2|Z|}}{2\pi} \left[|Z| \partial_Z^2 - 2Z \mathcal{G}(u) \partial_Z \right] \\
\mathcal{G}(u) &\equiv 7 - \frac{4}{1+u} - \frac{192u}{24(1+u) - \pi^2} \quad (3.22)
\end{aligned}$$

Thus the first order Hamiltonian and zeroth order eigenfunctions are sufficient to determine the eigenvalue and hence the mass up to first order in δ .

Note that the determination of mass requires us to solve (3.14) for which we need to perform an integral over all Z . However, due to normalizability of the eigenfunctions, the integrand contributes insignificantly for large Z . On the other hand, by taking r_c small, Z integration will be dominated by Region I. Thus, we conclude that choosing IR cutoff r_c arbitrarily small, the meson spectrum can be made independent of Region II and Region III and thus insensitive to UV modes of the gauge theory. Now of course we cannot choose r_c arbitrarily small, since then we need to consider deformed, resolved cone and our analysis do not apply. However, the normalizability of eigenmodes suggest that even for reasonably large r_c , the mass computation will be dominated by Region I. This is not surprising since meson physics is a low energy affair and UV effects can leave the IR intact.

3. Mesons Identification

We would like to verify if this effective model of large N QCD shares even more similarities with the experiments by comparing ratios of m_n^2 of well-known vector mesons. In order to do so, we must first identify which kind of mesons are present in this effective theory by looking at their behavior under charge conjugation (\mathcal{C}) and parity (\mathcal{P}). Parity operator is a Lorentz transformation flipping the space-like coordinates while charge conjugation corresponds to a flip of the Z coordinate[15]. Looking at the expansion of the four-dimensional gauge potential (3.10), we conclude that $B_\mu^{(n)}$ must be odd (resp. even) under parity/charge conjugation when α_n is even (resp. odd) in order for A_μ to behave as a 4-vector and acquire an overall sign under charge conjugation.

Knowing the eigenvalues of each vector mesons under \mathcal{P} and \mathcal{C} , we can identify them using the Particle Data Group (PDG) database [9] where we use their mass measurements M_{PDG} for comparison. Also, we concentrate on fields that are vectors of the approximate isospin $SU(2)$ symmetry as it was clarified in [13]. In table I we summarize our knowledge of each vector mesons $B_\mu^{(n)}$ both at zeroth and first order in $\delta = g_s M^2/N$.

Although the results to first order in δ presented in table I are slightly better than the ones of Sakai-Sugimoto [15] and others [18], so far the discussions have been confined to the massive KK modes of the *massless* open string sector of the theory. However open strings also have massive modes, and in principle these modes can also be identified as mesons. As an example, in table I, the 1^{--} states $\rho(1450)$ and $\rho(1700)$ could also appear from the massive stringy sector of the model. For AdS space an analysis has been performed in [17], where it was shown that the vector meson spectra do get contributions from the massive stringy modes. A similar analysis for our case is rather hard to perform

TABLE I. Mass ratio predictions with $0 < \delta < 0.4$ and a maximal correction of 70%; $\delta = 0.4000$ and $u = 0.0528$ minimize $\chi^2/2$ to 1.4200. Results are compared with both Sakai-Sugimoto [15] and PDG values [9].

	λ_n/λ_m	Sa-Su	$R_{n/m}^{(0)}$	$R_{n/m}^{(1)}$	$R_{n/m}^{\text{PDG}}$
$m_{a_1(1260)}^2/m_{\rho(770)}^2$	λ_2/λ_1	2.32	2.54	2.34	2.52
$m_{\rho(1450)}^2/m_{\rho(770)}^2$	λ_3/λ_1	4.22	5.27	4.19	3.57
$m_{a_1(1640)}^2/m_{\rho(770)}^2$	λ_4/λ_1	6.62	8.51	6.14	4.51
$m_{\rho(1700)}^2/m_{\rho(770)}^2$	λ_5/λ_1	9.53	12.95	8.46	4.92

because RR states do not decouple in the simple way as in [17], rendering the quantization procedure highly non-trivial. This means a definite predictions cannot be made at this stage. Thus for our case we will continue to use the massless open string sector to study the vector mesons. The other three states appearing in table I, namely $1^{--}[\rho(770)]$, $1^{++}[a_1(1260)]$ and $1^{++}[a_1(1640)]$, are only from the massless open string sector. In addition to that, the massless open string sector cannot be identified with scalar mesons of QCD, since a certain Z_2 symmetry is not shared by the theories as pointed out in [17]. Thus our analysis is limited to the study of vector mesons. More details on scalar meson including its

spectrum will be given in [3].

IV. CONCLUSION

In this note, we have summarized a proposal for a brane configuration and the dual geometry that can mimic several features of large N QCD. For the first time using a top-down model where classical description is sufficient, we are able to reproduce some aspects of RG flow and vector meson spectrum that are consistent with QCD. Our study of normalizable modes on probe branes suggests that vector mesons heavier than the deconfinement scale but lighter than Λ_0 (above which the theory is almost CFT) are independent of UV ($\Lambda > \Lambda_0$) physics. By choosing two parameters, we can predict four mass ratios and the results show considerable improvement over previous similar approaches in reaching agreement with experimental data. Although there are many similarities, the brane theory cannot be identified with QCD. Rather the holographic techniques should be best utilized as tools to gain analytic understanding of the non-perturbative regimes of QCD.

Acknowledgements: It is a great pleasure to thank Shigeki Sugimoto, Peter Ouyang and Martin Kruczenski for helpful discussions. The work of K. D., C. G., M. R., and O. T. is supported in part by the Natural Sciences and Engineering Research Council of Canada, and that of M. M is supported in part by DOE grant number DE – SC0007884.

-
- [1] J. M. Maldacena, Adv. Theor. Math. Phys. **2**, 231 (1998) [hep-th/9711200].
- [2] I. R. Klebanov and M. J. Strassler, JHEP **0008**, 052 (2000) [hep-th/0007191].
- [3] K. Dasgupta, C. Gale, M. Mia, M. Richard and O. Trotter, *in preparation*.
- [4] I. R. Klebanov and E. Witten, Nucl. Phys. B **536**, 199 (1998) [hep-th/9807080].
- [5] M. Mia, Phys. Rev. D **89**, 043010 (2014) [arXiv:1307.7732 [hep-th]].
- [6] M. Mia, K. Dasgupta, C. Gale and S. Jeon, Nucl. Phys. B **839**, 187 (2010) [arXiv:0902.1540 [hep-th]].
- [7] M. Mia, K. Dasgupta, C. Gale and S. Jeon, Phys. Rev. D **82**, 026004 (2010) [arXiv:1004.0387 [hep-th]].
- [8] M. Mia, F. Chen, K. Dasgupta, P. Franche and S. Vaidya, Phys. Rev. D **86**, 086002 (2012) [arXiv:1202.5321 [hep-th]].
- [9] J. Berenger *et al.* [Particle Data Group Collaboration], Phys. Rev. D **86**, 010001 (2012).
- [10] S. W. Hawking and D. N. Page, Commun. Math. Phys. **87**, 577 (1983).
- [11] E. Witten, Adv. Theor. Math. Phys. **2**, 505 (1998) [arXiv:hep-th/9803131].
- [12] M. Mia and F. Chen, JHEP **1301**, 083 (2013) [arXiv:1210.3365 [hep-th]].
- [13] D. T. Son and M. A. Stephanov, Phys. Rev. D **69**, 065020 (2004) [hep-ph/0304182].
- [14] S. Kuperstein, JHEP **0503**, 014 (2005) [hep-th/0411097].
- [15] T. Sakai and S. Sugimoto, Prog. Theor. Phys. **113**, 843 (2005) [hep-th/0412141].
- [16] T. Sakai and S. Sugimoto, Prog. Theor. Phys. **114**, 1083 (2005) [hep-th/0507073].
- [17] T. Imoto, T. Sakai and S. Sugimoto, Prog. Theor. Phys. **124**, 263 (2010) [arXiv:1005.0655 [hep-th]].
- [18] M. Kruczenski, D. Mateos, R. C. Myers and D. J. Winters, JHEP **0307**, 049 (2003) [hep-th/0304032]; M. Ihl, M. A. C. Torres, H. Boschi-Filho and C. A. B. Bayona, JHEP **1109**, 026 (2011) [arXiv:1010.0993 [hep-th]]; A. L. Cotrone, A. Dymarsky and S. Kuperstein, JHEP **1103**, 005 (2011) [arXiv:1010.1017 [hep-th]].
- [19] The resolved deformed cones, with or without squashing, are not Calabi-Yau manifolds but more general non-Kähler manifolds.
- [20] The deformed conifold is characterized by non-zero size of S^3 at base of the conifold, which in turn determines the scale of confinement. The size corresponds to expectation values of gauge invariant combinations of bifundamental fields and gives a length scale. If r_c is bigger than this length scale, then the cutoff geometry can be identified with $r > r_c$ regions of deformed cone.